Wall friction and boundary layer development in the cone of a Francis turbine scale model

Author	Firm / Institution	City, Country	Lecturer (x)
Elena-Lavinia Berca *Gabriel Dan Ciocan* *François Avellan*	*Laboratory for Hydraulic Machines* *Swiss Federal Institute of Technology Lausanne*	*Lausanne, Switzerland*	*x*

Abstract

To characterize the boundary layer development, in the cone of the Francis turbine, wall friction and velocity measurements are performed. The mean wall friction measurements evidence the increasing risk of the boundary layer separation at the cone wall with the increase of the discharge. The flow surveys close to the wall evidence a development of a 3D boundary layer under adverse pressure gradient. The analysis of the results reveals that the composite power law of *Barenblatt and Chorin* is a good approximation for the velocity profiles in the near wall region for the 4 operating points considered.

Résumé

La caractérisation de l'évolution de la couche limite dans le cône d’une turbine de Francis, est réalisée à partir des mesures de frottement pariétal et de vitesse. Les mesures de frottement pariétal moyen indiquent un risque accru de décollement de la couche limite dans le cône avec l'augmentation du débit Le relevé de vitesse au voisinage de la paroi met en évidence le développement d'une couche limite tridimensionnelle soumise à un gradient de pression adverse. L'analyse des résultats révèle que la loi composite de puissance de *Barenblatt and Chorin* est une bonne approximation des profils de vitesse proche de la paroi pour les 4 points de fonctionnement considérés.

Nomenclature

E	Specific energy	[J/Kg]	y	Distance from the wall	[m]
H	Piezometric head	[m]	y^+	Dimensionless distance from the wall	[-]
Re_θ	Reynolds number based on momentum displacement thickness	[-]	φ	Discharge coefficient $\varphi = \dfrac{Q}{\pi \cdot \omega \cdot (D_{1e}/2)^3}$	[-]
Q	Discharge	[m^3/s]	κ	Von Karman constant	[-]
U_∞	Mean flow velocity	[m/s]	ν	Kinematic viscosity	[m^2/s]
N	Rotational speed	[rpm]	θ	Momentum displacement	[m]

				thickness	
n_q	Specific speed $n_q = \varphi^{1/2} / \psi^{3/4}$	[-]	ρ	Fluid density	[kg/m^3]
u	Flow velocity	[m/s]	τ_p	Wall friction	[Pa]
u^+	Dimensionless velocity	[-]	ω	Rotational pulsation	[rad/s]
u_τ	Friction velocity	[m/s]	ψ	Specific energy coefficient $\psi = \frac{2 \cdot g \cdot H}{\omega^2 \cdot (D_{\bar{1}e} / 2)^2}$	[-]

Introduction

The challenging problem in fluid mechanics, nowadays, is still the control of the behavior of the turbulent boundary layers, with regard to their separation or detachment. Von Karman and Prandtl are the first, since 1930, who proposed a model for the turbulent boundary layer. Their model describes the wall region by means of a universal logarithmic law, by assuming that outside the viscous sub layer, the contribution of viscosity can be neglected. In 1950, *Clauser* [Ref 8] and *Coles* [Ref 9] proposed a model for turbulent boundary layers at large Reynolds number, based on the assumption that the transition from the wall region, described by Karman-Prandtl law, to the external flow, called “wake region”, is smooth. This model, called classical, is widely accepted and used, especially for the zero-pressure gradient turbulent boundary layer.

Using analytic and experimental arguments, since 1991, *Barenblatt and al.* [Ref 3] developed a new and different model, which contradicts the classical theory. This model shows that the intermediate region in turbulent boundary layers at large Reynolds number, between the viscous sub-layer and the external flow consists on two self-similar structures, described by different and substantially Reynolds-number-dependent scaling laws. However, the boundary between them is sharp. In fact, according to this model, the mean velocity profile in the transition region has a characteristic form of a “chevron”. This model was validated for both zero-pressure and non- zero-pressure gradient flows.

The recent progresses in the boundary layer investigation show that, for the flows with adverse pressure gradient, the standard log-law velocity profile does not hold, near-wall distributions of r.m.s. velocity fluctuations cannot by scaled with the wall parameters, friction velocity and kinematic viscosity and that the response time of turbulence to the imposed adverse-pressure-gradient, differs among streamwise wall-normal and spanwise velocity components.

In Francis turbine the evolution of the boundary layer in the cone is complex due to the rotating flow at the runner outlet, the adverse pressure gradient, the interaction with the leakage flow and the unsteady perturbations due to the runner blade-to-blade shared flow or vortex rope.

This paper intents to present the experimental setup for wall friction measurements and near wall velocity measurements in the cone of a Francis turbine scale model. The boundary layer is characterized and the best-fitted model is provided for the boundary layer model. Meanwhile, the boundary layer thicknesses are determined for the cone inlet and outlet, for different spatial positions and for 4 operating points of the turbine .

Experimental setup

In the framework of FLINDT, Flow Investigation in Draft Tubes, research project, EUREKA no. 1625, the wall friction measurements are performed in the cone of a $\nu = 0.56$, $n_q = 92$, industrial high specific speed Francis turbine scale model, see Figure 1.

The global measurements of flow, specific energy and efficiency are performed according to *IEC* recommendations [Ref 15] at the EPFL, Laboratory for Hydraulic Machines. Four operating points are selected to characterize the central part of draft tube characteristics for $\psi = 1.18$ and: $\varphi_A = 0.340$, $\varphi_B = 0.368$, $\varphi_C = 0.380$, $\varphi_D = 0.410$, Figure 2. The model characteristics and the selected operating points are described in *Avellan* [Ref 1].

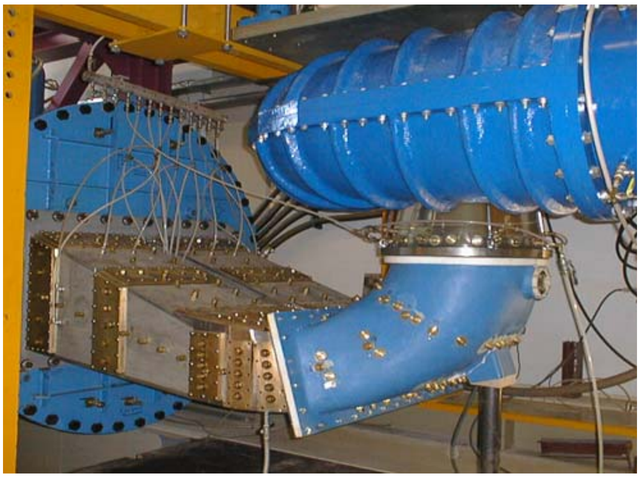

Figure 1 FLINDT Francis turbine scale model.

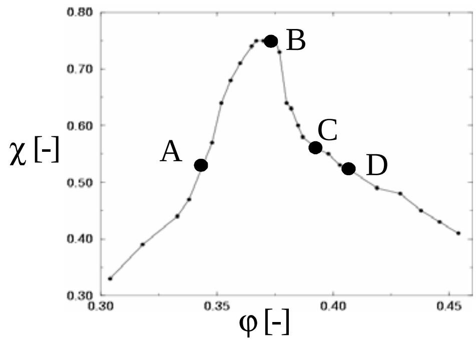

Figure 2 Draft tube pressure recovery

Wall friction measurements

For the wall friction measurements, two sections are investigated, at the inlet and at the outlet of the turbine model cone, Figure 3. In order to study the wall friction distribution with the angular position, the hot-film probe is embedded in the cone; see Figure 4, for the inlet at 9 different locations, and for the outlet, at 7 different locations.

The wall friction measurements are performed using a flush mounted hot-film probe, 55R46, produced by DANTEC Measurement Technology, together with a Constant Temperature Anemometer. The main technical data for the 55R46 flush mounted hot-film probe used are presented, Table 1.

The calibration of the hot-film probe is performed in the water tunnel of the EPFL Laboratory for Hydraulic Machines. The procedure and the influence of the calibration parameters over the measurements are presented in *Ciocan and al.* [Ref 5]. Using this procedure for the wall friction measurement that inlcudes all the error factors correction, a global accuracy of 5% of the measured value is obtained. The calibration of the sensor with respect this accuracy if the unsteady flow angle fluctuations are less that $^{+}/_{-}8°$ compared to the sensor direction.

Table 1 Hot-film sensor characteristics

Thickness of quartz coating	Sensor material	Sensor dimensions	Sensor resistance R_{20}	Leads resistance	Temperature coefficient of resistance (TCR) α_{20}	Max. sensor temperature	Frequency limit f_{cpo}
2µm	*Nickel*	*0,75x0,2 mm*	*11,9Ω*	*1,4Ω*	*0,47%/C*	*150°C*	*30kHz*

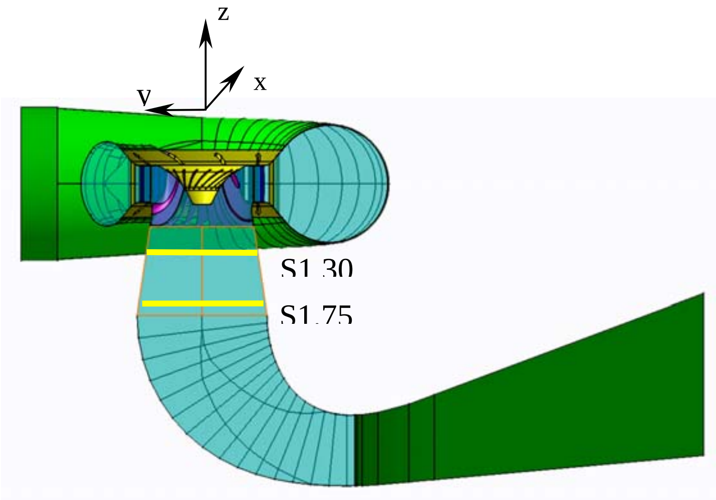

Figure 3 Wall friction measurement sections.

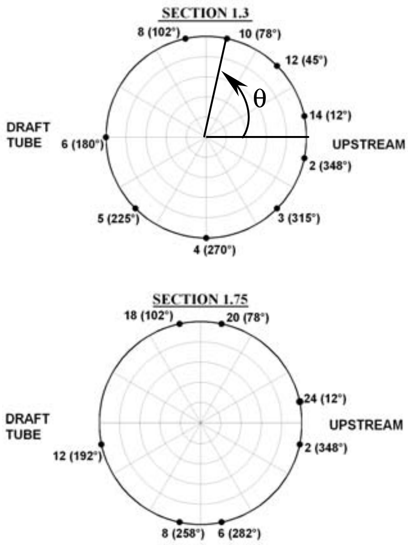

Figure 4 Location of the wall friction sensors

Near wall 2D LDV measurements

To complete the boundary layer analysis, a 2D velocity profile survey is performed near the cone wall by LDV measurement method. The LDV system is a Dantec 2 components system, using back-scattered light and transmission by optical fiber, with a laser of 5W Argon-ion source. The main characteristics of the LDV probe are detailed, Table 2.

Table 2 Main optical probe characteristics

	Laser wave lengths	Probe diameter	Beam spacing	Focal length	Fringe spacing	Measuring Volume $\sigma_x = \sigma_y$	Measuring Volume σ_z
LDV probe	*488 nm 514.5 nm*	*60 mm*	*~38 mm*	*159.4 mm*	*~2.15 nm*	*~0.1 mm*	*~0.8 mm*

An optical window with plane and parallel faces is used as interface. The geometrical reference position of the measurements is obtained by positioning the laser beams on the windows faces with an accuracy of better than 0.05 mm.

Two components are measured: the tangential component of the velocity c_x and the axial one c_z, see Figure 5. An exploration of the complete diameter of the cone was already performed; see Ciocan and al. [Ref 6] and the comparison of the near wall measurements with the velocity profile showed a very good agreement, see Figure 6. The uncertainties of the laser measurements are estimated to 2%, according to the method of *Mofat et al.* [Ref 14].

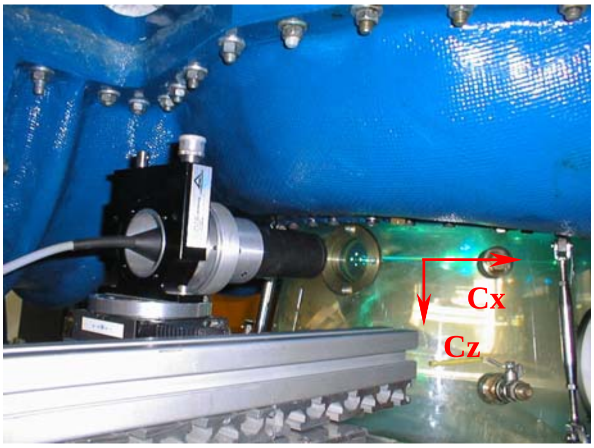

Figure 5 Near wall LDV measurements.

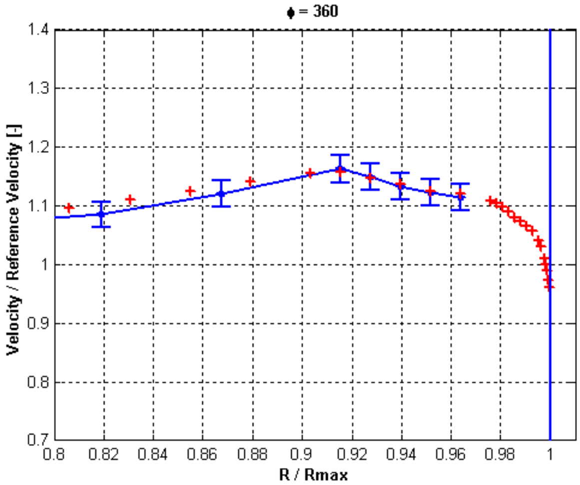

Figure 6 Velocity distribution in the cone near wall region

Wall friction results

For the steady analysis it is presented a comparison between the distribution of the mean wall friction related to the operating points and the angular position of the probe in the 2 sections, see Figure 7.

For each operating point the repartition is quite uniform. At the cone outlet, the bend influence over the wall friction distribution is noticed. In fact, around 180° position, that corresponds to the bend position, the wall friction values are 25% less than the values corresponding to the upstream positions.

For the both sections, the same trend for the wall friction values is noticed: the wall friction decreases by increasing the mean flow velocity; this trend shows an increased separation risk of the boundary layer. The wall friction values at the cone outlet are about 1/3 of the exiting values at the cone inlet for all operating points.

It is also presented a comparison with the numerical results obtained by *Mauri* [Ref 13] for the boundary layers; see Figure 8, for the cone inlet section corresponding to 4 angular positions: 78°, 180°, 270° and 348°. The computed wall friction values are underestimated by about 25% and there is not a significant difference between the different angular positions.

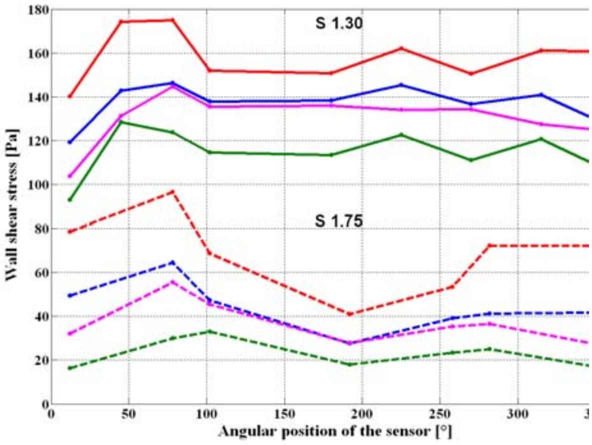

Figure 7 Angular distribution of the wall friction

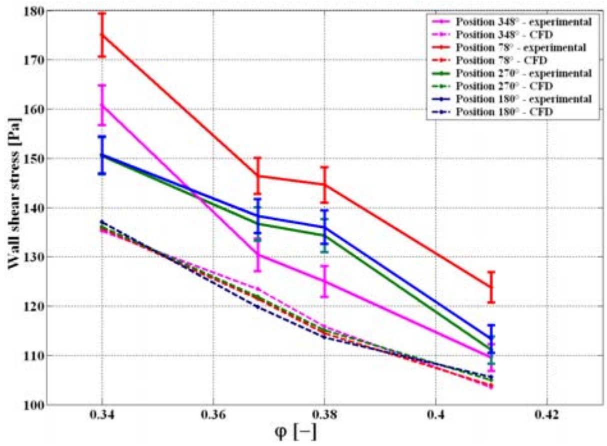

Figure 8 Wall friction distribution: experimental and CFD results

Near wall LDV results

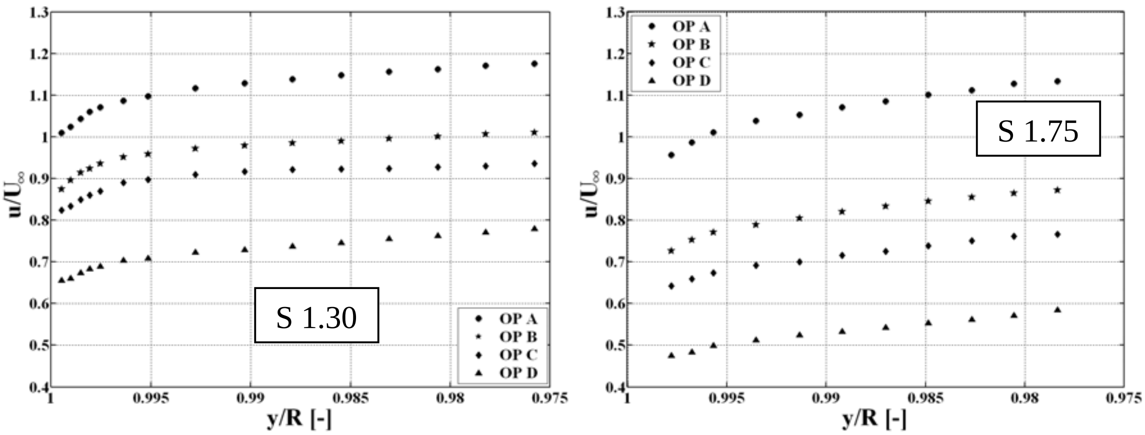

Figure 9 Near wall velocity measurements (y/R=1 corresponds to the wall)

The velocity measurements in the vicinity of the cone wall between 0.2 mm and 20 mm, see Figure 9, corresponding to y^+ values between ~100 and 10'000, will allow obtaining the boundary layer law.

Boundary layer analysis

Boundary layer representation

Using inner variables, u^+ and y^+, see (1) and the measured values of the wall friction and near wall velocity, the boundary layer can be represented for the inlet and outlet section of the cone, Figure 10.

$$u^+ = \frac{u}{u_\tau} \qquad u_\tau = \sqrt{\frac{\tau_p}{\rho}} \qquad y^+ = \frac{y u_\tau}{\nu} \qquad (1)$$

In Section 1.30, at 0.2 D_{1e} from the runner outlet, the boundary layer thickness and shape are very similar. In Section 1.75, at 0.6 D_{1e} from the runner outlet, due to the adverse pressure gradient values, see *Arpe* [Ref 1], the boundary layer thickness is proportional to the flow rate.

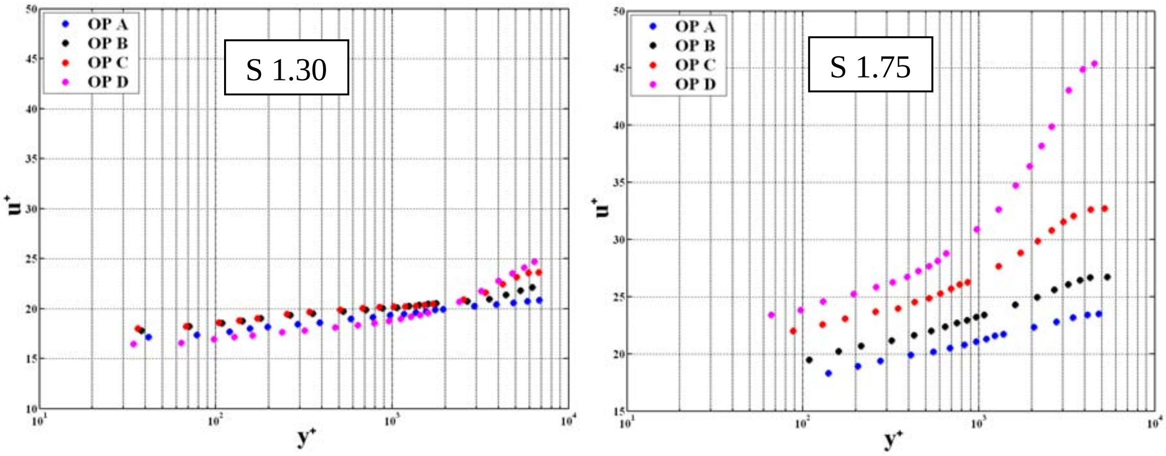

Figure 10   Velocity profile distribution expressed as boundary layer inner variables.

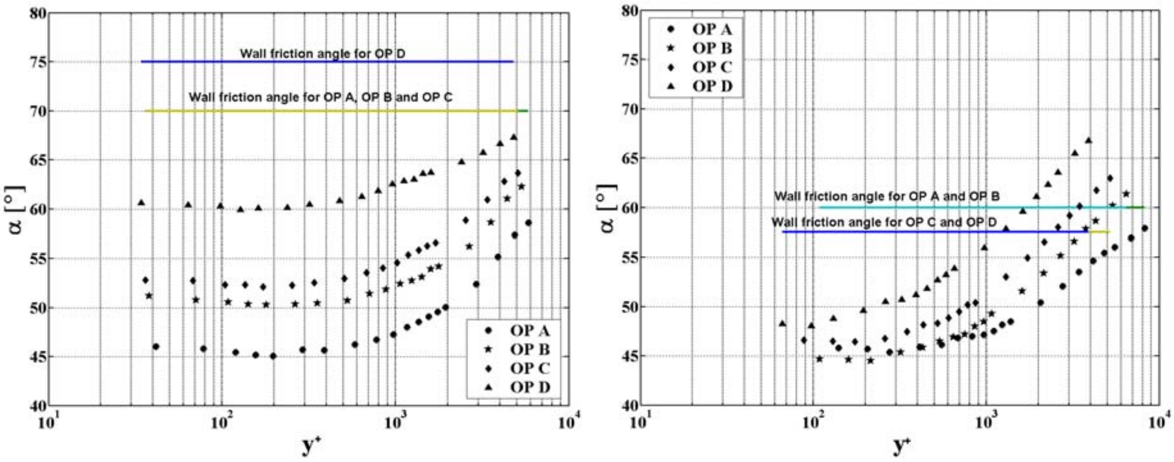

Figure 11   Flow angle distribution in the boundary layer.

Comparison with the classical model of boundary layer

The model of the turbulent boundary layer at large Reynolds number, proposed by the *Clauser* [Ref 8] and *Coles* [Ref 9], is based on the assumption that the velocity distribution in the intermediate region follows the Karman-Prandtl universal logarithmic law. The mean velocity distribution follows, according to this classical model, the universal logarithmic law:

$$u^+ = \frac{1}{\kappa}\ln y^+ + C \qquad (2)$$

where in general $\kappa = 0.41$ and $C = 5$.

The measurements results could be approximated with a logarithmic law but differences appear for the two constants values. The friction velocity based on the wall friction measurements is about 3 times larger than the one obtained with the classical log-law. This means, transformed in wall friction, that the ratio between the measured values and the calculated one is about 10.

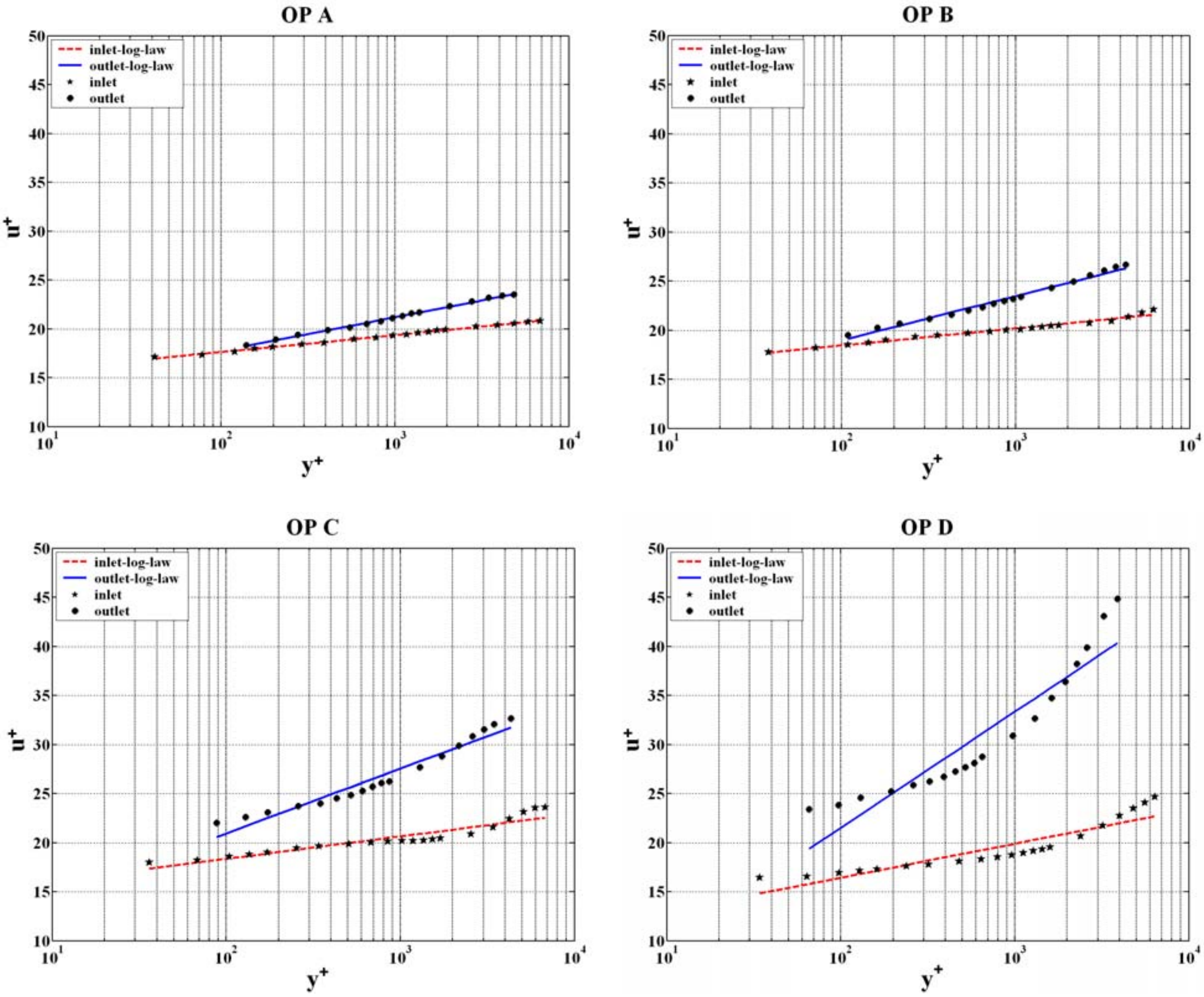

Figure 12 Comparison of the mean velocity distribution with the operating point.

In this way, it is noticed that using the log-law, see Figure 12, the boundary layer shape is inadequately approximated and in the some time the Karman-Prandtl universal logarithmic law is not valid for the turbine cone flow conditions.

The boundary layer in the Francis Turbine cone is strongly three-dimensional. The absolute flow angle representation, related to the local system attached to the hot-film probe, x' and z', for the LDV velocity field, shows a strong gradient in the boundary layer – see Figure 13.

Two supplementary raisons can be evocated and future studies are necessary to investigate this topic. The flow leakage at the runner outlet can produce a local separation and after the reattachment, in the measure section, the boundary layer is disturbed. The second one is the full turbulent mixed shear flow in the cone; see Iliescu and al. [Ref 12], that can have an impact on the boundary layer structure and measurement accuracy.

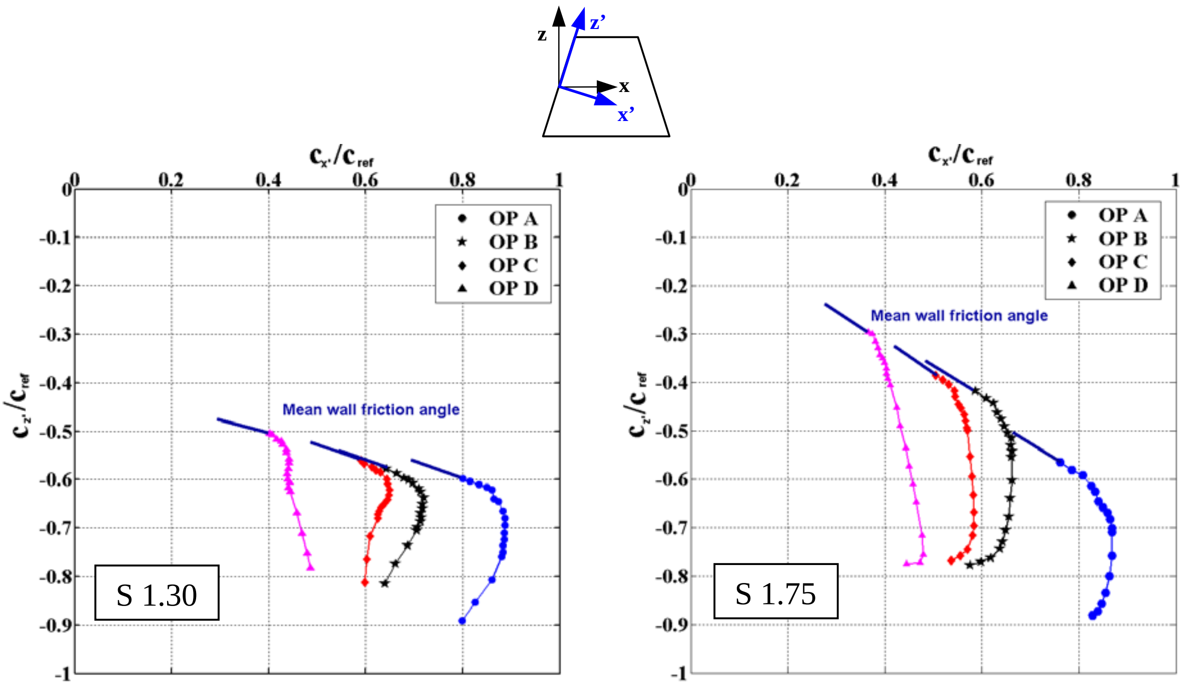

Figure 13 Flow angle variation in the boundary layer as compared with the friction angle

Superposed with the three-dimensionality, an adverse pressure gradient, see Arpe [Ref 1], is governing the flow, and its influence is clearly visible for $y^+ > 10^3$.

Comparison with the power model of boundary layer

According to a model of the turbulent boundary layer proposed by *Barenblatt and Chorin* [Ref 3], in the absence of the external turbulence, the transition region between the viscous sublayer and the external flow is composed by 2 sharply separated self-similar structures where the velocity distribution follows 2 different scaling laws. Actually, the characteristic form of the velocity distribution in this region is a broken line called “chevron”.

In the adjacent part to the viscous sub the scaling law describes layer the mean velocity distribution:

$$\Phi = A(\eta)^{\alpha} \qquad (3)$$

While in the other one, adjacent to the free stream, the scaling law becomes:

$$\Phi = B(\eta)^{\beta} \qquad (4)$$

where:

$$\Phi = \frac{u}{u_\tau} \qquad (5)$$

$$\eta = \frac{y u_\tau}{\nu} \qquad (6)$$

The approximation with a power law shows a good agreement with the measured velocity profiles, corresponding to the 3D fully turbulent flow in adverse pressure gradient conditions taking place in a Francis turbine cone, see Figure 14.

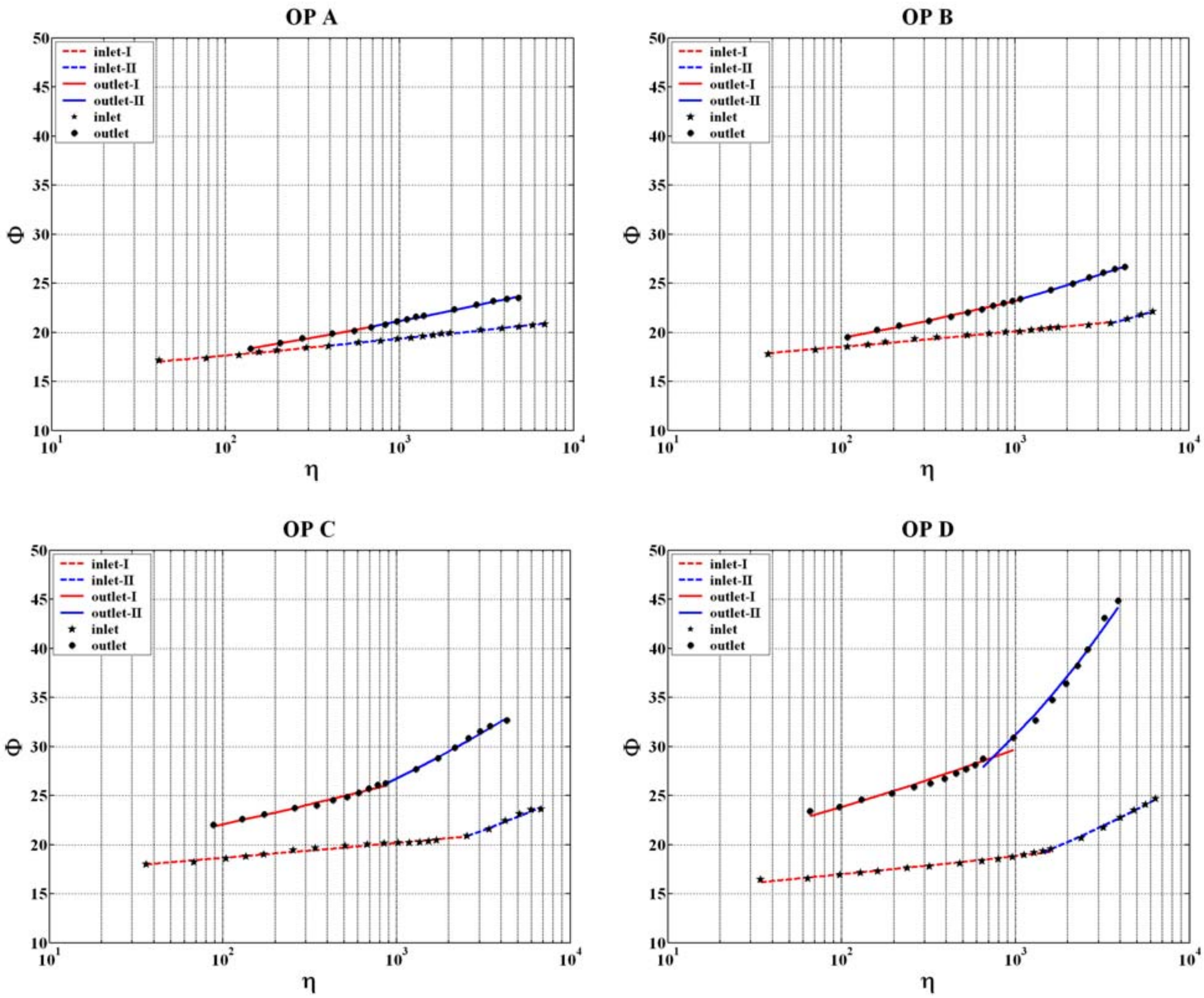

Figure 14 Boundary layer's "chevron" in the cone, both at the outlet and at the inlet, for each operating point

An interesting parameter of the flow, which influences the slopes of the mean velocity distribution is the Reynolds number based on the momentum displacement thickness; it has been calculated for each operating point:

$$\mathrm{Re}_\theta = \frac{\theta U}{\nu} \qquad (7)$$

The constants A, α, B and β are determined from the experimental data, Table 3, based on wall friction and near wall velocity measurements. The results are coherent with the *Barenblatt et al.* [Ref 3] analysis.

Table 1 The power scaling law constants

Operating point Section	Re□	A	α	B	β
A – S 1.30	*11'244*	*14.712*	*0.0394*	*14.727*	*0.0396*
B – S 1.30	*12'254*	*15.714*	*0.0356*	*9.4243*	*0.0976*
C – S 1.30	*14'444*	*15.923*	*0.0343*	*7.2035*	*0.1356*
D – S 1.30	*15'599*	*13.766*	*0.0455*	*5.7154*	*0.1666*
A – S 1.75	*8'983*	*13.041*	*0.0695*	*12.904*	*0.0715*
B – S 1.75	*13'992*	*13.567*	*0.0776*	*11.876*	*0.0970*
C – S 1.75	*17'309*	*15.530*	*0.0764*	*10.013*	*0.1422*
D – S 1.75	*21'810*	*15.319*	*0.0960*	*5.2872*	*0.2568*
I. Marušić (air)	*8'588*	*8.410*	*0.1450*	*5.6300*	*0.2070*

Conclusions

For an industrial scale model of Francis turbine, the boundary layers are characterized for an operating range in the vicinity of the best efficiency point. The coupled measurements of wall friction, by a hot film probe, and of velocity, by LDV in the near wall zone, allowed obtaining the boundary layer representation. The evolution of the boundary layer in the turbine cone is quantified.

The comparisons of the measured boundary layer with the von Karman-Prandtl universal logarithmic law showed that the classical model is not valid. The logarithmic law shape is existing but the constants are different. Two raisons are invocated and quantified: the strongly 3D character of the boundary layer and the adverse pressure gradient. Two other possible raisons: the runner outlet leakage flow and the unsteady character of the sheared flow must be investigated in the future. For the present case study, the composite power law of *Barenblatt and Chorin* gives a better description of the boundary layer for fully turbulent flow in adverse pressure gradient. Moreover, the validity for the wall law model, mostly used by the CFD RANS solver, should be reconsidered for the cone region of the Francis turbines, due to an underestimation of the friction values, see Mauri [Ref 13].

Acknowledgements

The authors would like to thank particularly all the partners of the FLINDT II Eureka Project No 1625, i. e. ALSTOM Hydro, EDF-CIH, GE Hydro, VA TECH Hydro, VOITH-SIEMENS Hydro Power Generation for their financial support and assistance. The FLINDT II project is funded by PSEL, Funds for Projects and Studies of the Swiss Electric Utilities, Contract award No 126, and CTI, Swiss Federal Commission for Technology and Innovation, Contract award No 5190.2 EUS. The authors would like also to thank gratefully the staff members of the EPFL Laboratory Hydraulic Machines, for their technical assistance.

References

Ref 1 Arpe J.A., "Experimental Investigation of Unsteady Pressure and Velocity Field in a draft tube of Francis Turbine*", EPFL Ph.D. Thesis No 2779*, 2003

Ref 2 Avellan F., “Flow Investigation in a Francis Draft Tube: the Flindt Project”, *Proceedings of the 20th IAHR Symposium, August 7-9 2000*, Charlotte, North Carolina, USA

Ref 3 Barenblatt G.I., Chorin A.J. and Prostokishin V.M. “A Model of a Turbulent Boundary Layer With a Non-Zero Pressure Gradient”, *Proc. Natl. Acad. Sci.USA, Applied Mathematics, 2002*

Ref 4 Barenblatt G.I., Chorin A.J., "Small viscosity asymptotics for the inertial range of local structure and for the wall region of wall-bounded turbulent shear flow", *Proc. Natl. Acad. Sci.USA, Applied Mathematics, vol.93, pp 6749-6752*,1996

Ref 5 Ciocan G.D., Avellan F., Berca E.L. “Wall Friction Measurements: Application in A Francis Turbine Cone”, *FEDSM2002-31333, , Joint US ASME – European Fluids Engineering Conference*, Montreal, Canada, 14-18 July 2002

Ref 6 Ciocan G.D., Avellan F., Kueny J.L. "Optical Measurement Techniques for Experimental Analysis of Hydraulic Turbines Rotor-Stator Interaction" *- ASME Fluid Engineering Conference,* 11-15 June 2000, Boston, USA

Ref 7 Ciocan G.D., Mauri S., Arpe J., Kueny J.L., "The Experimental and Numerical Study of the non stationary velocity field at the exit of a turbine runner" *La Houille Blanche no. 2,* 2001

Ref 8 Clauser F.H. J., "Turbulent Boundary Layers in Adverse Pressure Gradients", *Aero. Sci. 21, 91-108,* 1954

Ref 9 Coles D.E. J. "The law of the wake in the turbulent boundary layer", *Journal of Fluid Mechanics vol. 1 pp.91-108*, 1956

Ref 10 Goldstein R. J., "Fluid Mecanics Measurements", *Hemisphere Publishing Corporation*, 1983, USA

Ref 11 Iliescu M.S., Ciocan G.D., Avellan F. "3D PIV and LDV Measurements at the runner outlet of a Francis Turbine",*FEDSM2002-31332, Joint US ASME – European Fluids Engineering Conference,* Montreal, Canada, 14-18 July 2002

Ref 12 Iliescu M.S., Ciocan G.D., Avellan F. " Experimental Study of the Runner Blade-to-Blade Shear Flow Turbulent Mixing in the Cone of Francis Turbine Scale Model*", 22nd IAHR Symposium on Hydraulic Machinery and Systems,* June 29 – July 2, 2004 Stockholm, Sweden

Ref 13 Mauri S. "Numerical simulation and flow analysis of the elbow diffuser" – *EPFL thesis n°2527*, Lausanne, 2002

Ref 14 Mofat, R. J., "Using Uncertainty Analysis in Planning of an Experiment", *Journal of Fluid Engineering, Vol. 107 pp. 173-178*, 1985

Ref 15 ***, "Model acceptance tests to determinate the hydraulic performance of hydraulic turbines, storage pumps and pump-turbines", *International* Standard I.C.E., 1993